「Macromolecular Research」 목차

정기간행영문지_ 28권 1호 · 2020년 1월

COVER PAPER

3D-Printed Poly Lactic Acid Scaffolds with Tetrapod-Interlocked Structure Containing Dipyridamole

Dae-Ryong Jun, Guk-Young Ahn, In Seong Choi, Tae Hoon Yun, Kun Na, and Sung-Wook Choi*

Vol. 28, No. 1, pp 5-8 (2020) | JAN 25, 2020 | DOI 10.1007/s13233-020-8017-0

Poly lactic acid scaffold with a tetrapod-interlocked structure exhibited stronger compressive stress resistance than cubic or tetrapod scaffolds. By using the dipyridamole, the ability to proliferate osteoblast and inhibit osteoclast formation made the scaffold favorable to bone regeneration.

COMMUNICATIONS

Structure and Properties of Aromatic Polyimide Fibers Fabricated by a Novel "Reaction-Spinning" Method

Zhentao Li, Jie Dong*, Jian Huang, Tao Guo, Shihua Wang, Xin Zhao, and Qinghua Zhang*

Macromol. Res., **28**, 1 (2020)

High-performance polyimide fibers were successfully prepared by an environmentally-friendly "reaction-spinning" process, in which the solidification of spinning dope and partial imidization take place simultaneously. Thus, the stability of precursor fibers can be improved and microvoids in fibers can be greatly reduced compared to samples by the conventional two-step wet-spinning method. This novel technology is expected to be applicable in large-scale preparation of PI fibers.

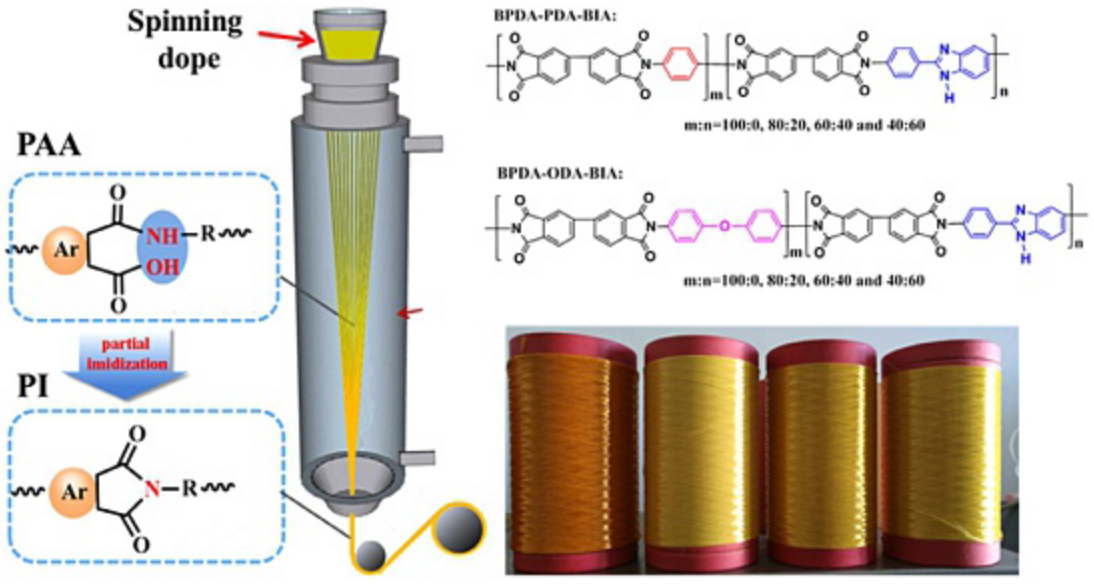

3D-Printed Poly Lactic Acid Scaffolds with Tetrapod-Interlocked Structure Containing Dipyridamole

Dae-Ryong Jun, Guk-Young Ahn, In Seong Choi, Tae Hoon Yun, Kun Na, and Sung-Wook Choi*

Macromol. Res., **28**, 5 (2020)

Cover Paper

Poly lactic acid scaffold with a tetrapod-interlocked structure exhibited stronger compressive stress resistance than cubic or tetrapod scaffolds. By using the dipyridamole, the ability to proliferate osteoblast and inhibit osteoclast formation made the scaffold favorable to bone regeneration.

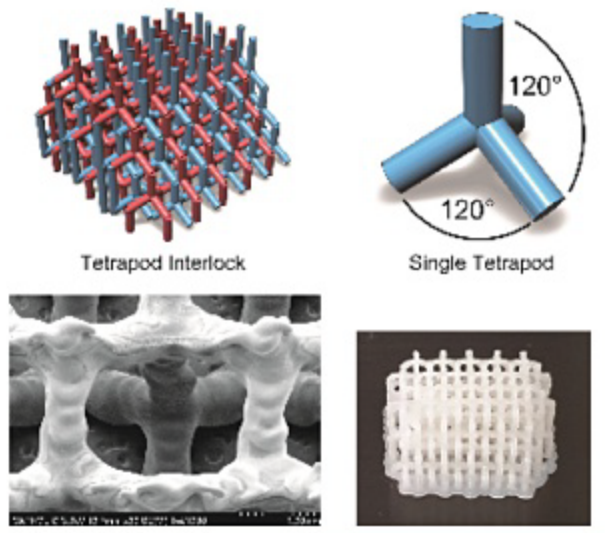

ARTICLES

Poly-L-lactide Polymer-Based Triple Drug-Eluting Stent with Abciximab, Alpha-Lipoic Acid and Sirolimus in Porcine Coronary Restenosis Model

Jun-Kyu Park, Sung Soo Kim, Hyun Kuk Kim, Jae-Woon Nah, Han Byul Kim, In Ho Bae, Dae Sung Park, Jae Won Shim, Min Young Lee, Joong Sun Kim, Bon-Sang Koo, Kang-Jin Jeong, Yeong Bae Jin, Sun-Uk Kim, Sang-Rae Lee,Joo-Young Na, Doo Sun Sim, Young Joon Hong, Kyung Seob Lim*, and Myung Ho Jeong*

Macromol. Res., **28**, 9 (2020)

Poly-L-lactide is a biocompatible and biodegradable polymer for coating the medical device. This is the first preclinical study to evaluate the effect of poly-L-lactide polymer based triple drug-eluting stent with antithrombotic abciximab,antioxidative alpha-lipoic acid, and antiproliferative sirolimus in porcine coronary restenosis model. Our study shows that novel triple drug-eluting stent inhibited coronary inflammatory reaction and neointima hypearplaisa compared to sirolimus-eluting or bare metal coronary stent at 1 month after stent implantation in a porcine coronary restenosis model. Therefore, synergy effects of triple drugs can be a feasible drug combination for manufacturing of futuristic coronary stent.

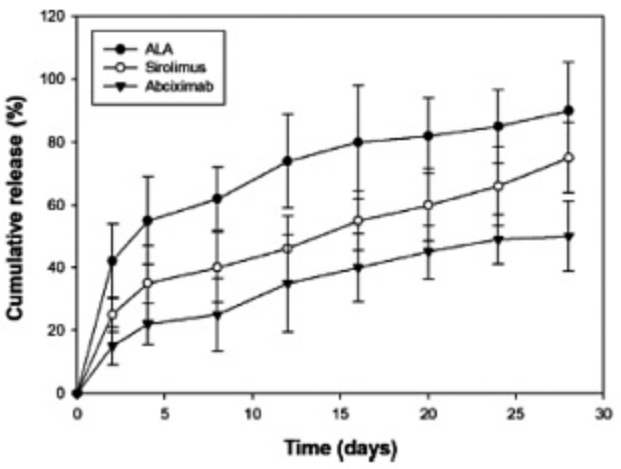

Surface Properties of Structure-Controlled Silica Films Prepared Using Organic-Inorganic Hybrid Solutions

John Magak Otieno, Nahae Kim, Ho Sun Lim*, and Juyoung Kim*

Macromol. Res., **28**, 15 (2020)

Poly(urethane acrylate nonionomer) (PUAN) was used as an amphiphilic polymer to prepare various organic-inorganic (O-I) hybrid solutions. The PUAN concentration in the O-I hybrid solutions was varied to control microphase separation to form various microstructures in the silica films. We achieved a suitable surface roughness that resulted in both high hydrophobicity and excellent mechanical robustness. We use a reproducible method that avoids high-aspect-ratio protrusions that can be prone to erosion and wear. Such structures are expected to be suitable for A, B, and C applications.

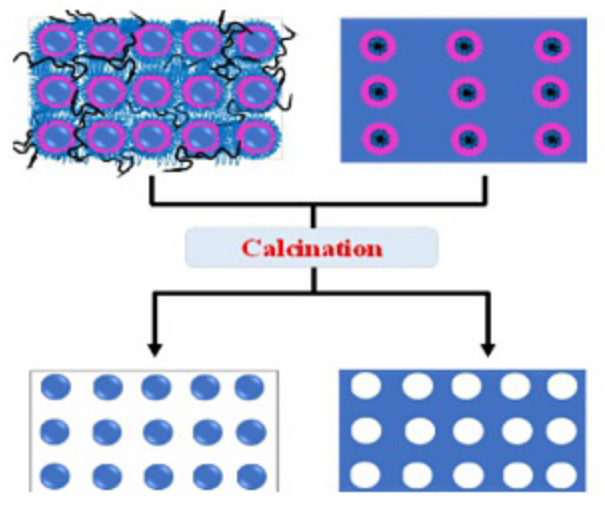

Improvement of Biodegradability and Biocompatibility of Electrospun Scaffolds of Poly(butylene terephthalate) by Incorporation of Sebacate Units

Nina Heidarzadeh, Luis J. del Valle*, Lourdes Franco, and Jordi Puiggalí*

Macromol. Res., **28**, 23 (2020)

Electrospinning of single solutions of poly(butylene terephthalate) (PBT) and poly(butylene sebacate-*co*-terephthalate) (PBSeT) mixtures and co-electrospinning of independent PBT and PBSeT solutions. Hydrolytic and enzymatic degradation studies demonstrated the success of the approach due to the susceptibility of the PBSeT component towards the enzymatic attack with lipases from *Pseudomonas cepacia* and even towards high temperature hydrolysis.

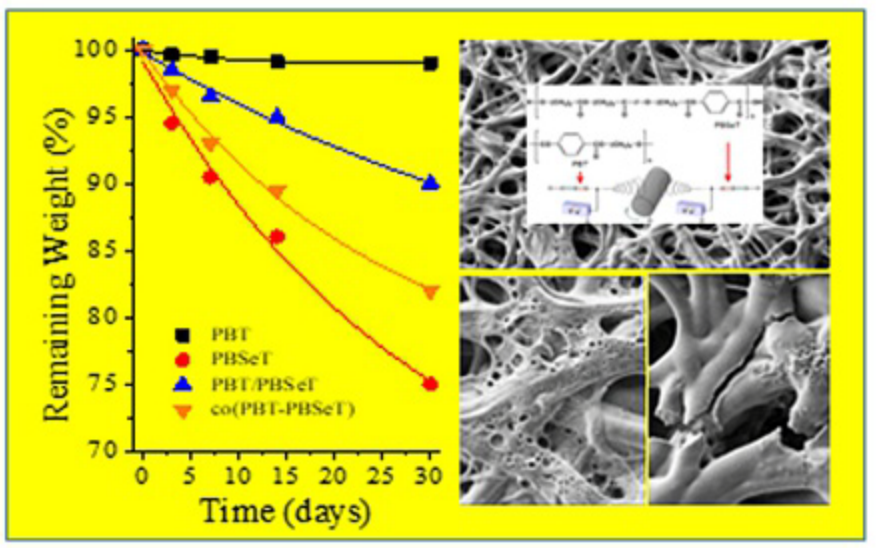

Carbon-Fiber-Reinforced Epoxy Resin with Sustainable Additives from Silk and Rice Husks for Improved Mode-I and Mode-II Interlaminar Fracture Toughness

Cuong Manh Vu, Quang-Vu Bach*, Huong Thi Vu, Dinh Duc Nguyen, Bui Xuan Kien, and Soon Woong Chang

Macromol. Res., **28**, 33 (2020)

The mode II interlaminar fracture toughness values increased with increasing crack length. It is not hard to realize the incorporation of hybrid fillers, SiO_2 and silk fibroin nanofiber (nSF), to help improve the mode II interlaminar fracture toughness (G_{IIC}) of the carbon fiber-reinforced epoxy resin (CFRE). G_{IIC} was increased by 30.06%, from 1350 to 1756 kJ/m^2, when the pristine composite sample was replaced with a modified CFRE containing 20:0.2 (w/w) SiO_2/nSF. The mechanisms for enhancing G_{IIC} include de-bonding, bridging, fiber pullout, as well as the fracturing of the matrix and fibers.

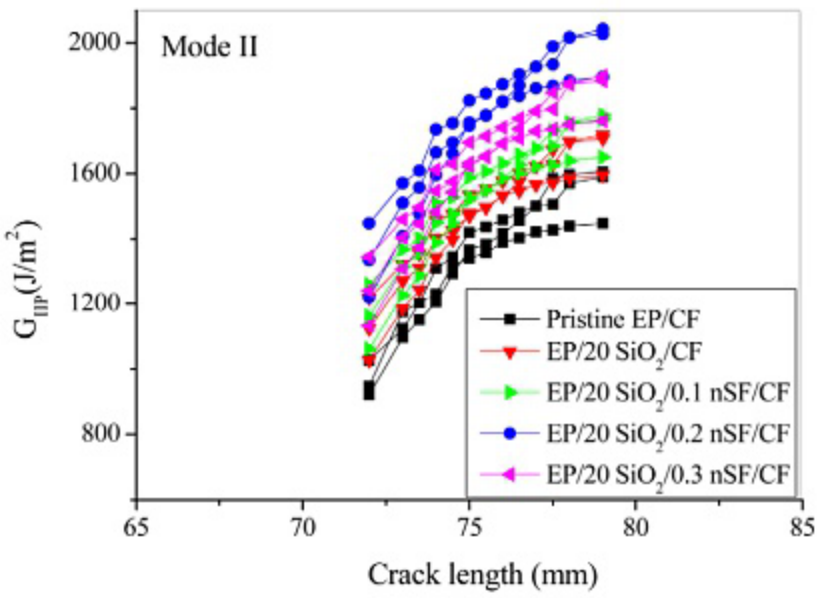

Investigation of UiO-66 as Flame Retardant and Its Application in Improving Fire Safety of Polystyrene

Wenling Chen, Yong Jiang*, Rong Qiu, Wu Xu, and Yanbei Hou

Macromol. Res., **28**, 42 (2020)

Zr-based metal-organic framework (UiO-66) was added into polystyrene (PS) as flame retardants (FRs) for the first time. It was found that UiO-66 could improve the flame retardation and smoke-suppression abilities of PS composites. The peak heat-release rate and total heat release values reduced by 26.8% and 14.7%, respectively comparing to those of pure PS. Meanwhile, a more than 35% reduction in total smoke production was achieved.

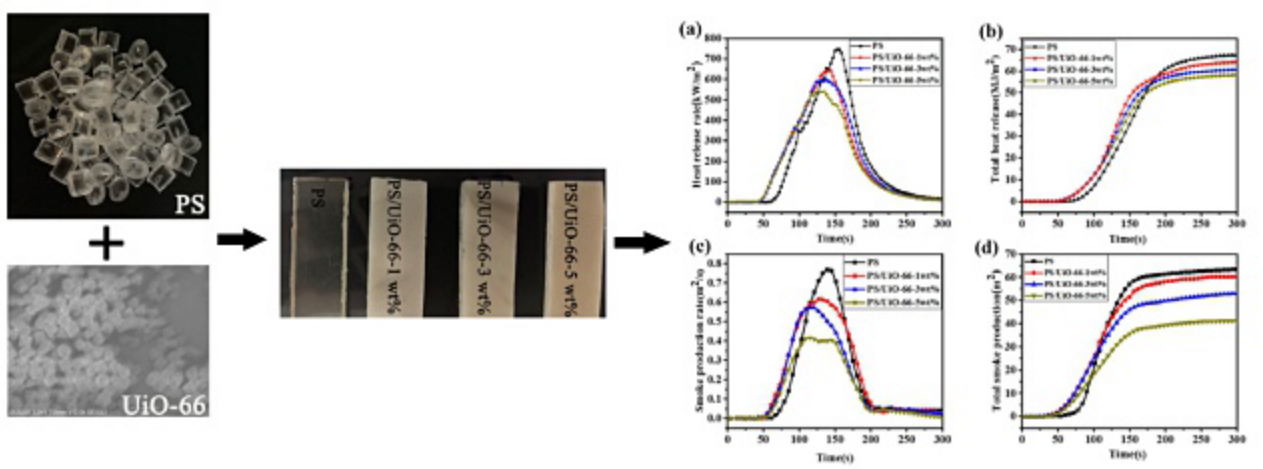

A Selective Colorimetric Sensor for Pb^{2+} Detection by Using Phenylboronic Acid Functionalized Polydiacetylene Liposomes

Siyu Zhang, Baoli Shi,
and Guang Yang*

Macromol. Res., **28**, 51 (2020)

Upon adding various metal ions into the liposome solution, only Pb^{2+} could cause a distinct color change from blue to red and a dramatic fluorescence enhancement with a fast response time in this sensor, which is prepared from a mixture of 4:1 (mol/mol) 10,12-pentacosadiynoic acid (PCDA) and phenylboronic acid (pBA) monomers.

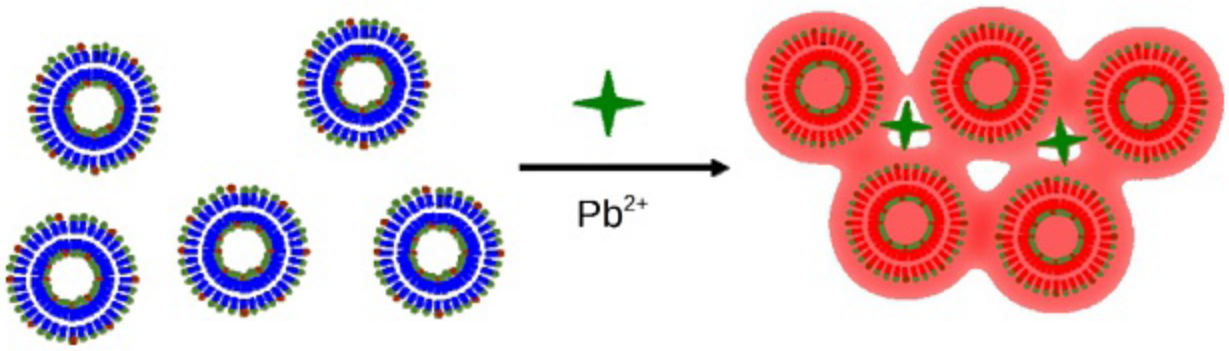

Leaf-Inspired Micro- and Nanoengineered Surfaces for Controlled Hydrophilic and Hydrophobic Properties

Daun Kim, Woochan Kim, Sunho Park,
Sujin Kim, Yonghyun Gwon,
and Jangho Kim*

Macromol. Res., **28**, 57 (2020)

We report on a simple, tunable replication method that mimics the unique surface of micro- and nanotopographies of common camellia, fragrant plantain, and lotus leaf, with properties that range from hydrophilic to hydrophobic. Using the lithographic technology in combination with thermal- or ultraviolet-sensitive materials, we engineered both hydrophilic and hydrophobic surfaces on a single material.

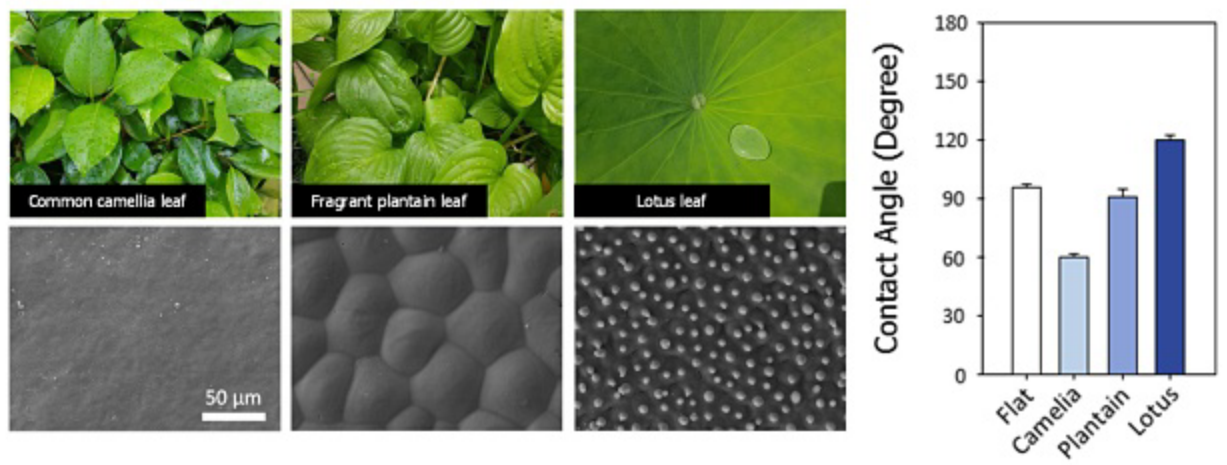

Effect of Head Structure on ATP Detection in Polydiacetylene Systems

Minhee Kim, Narae Han,
Min Jae Shin*, Min Kim*,
and Jae Sup Shin*

Macromol. Res., **28**, 62 (2020)

ATP detection systems were formed using 10,12-pentacosadiynoic acid derivatives that had a tertiary amine group. Ortho, meta, and para derivatives were synthesized and the receptiveness for ATP was characterized. Only the meta derivative showed a color change from blue to red upon ATP detection. The concentration of ATP that was able to be detected by the naked eye was 100 μM, and that by the UV spectrum was 50 μM.

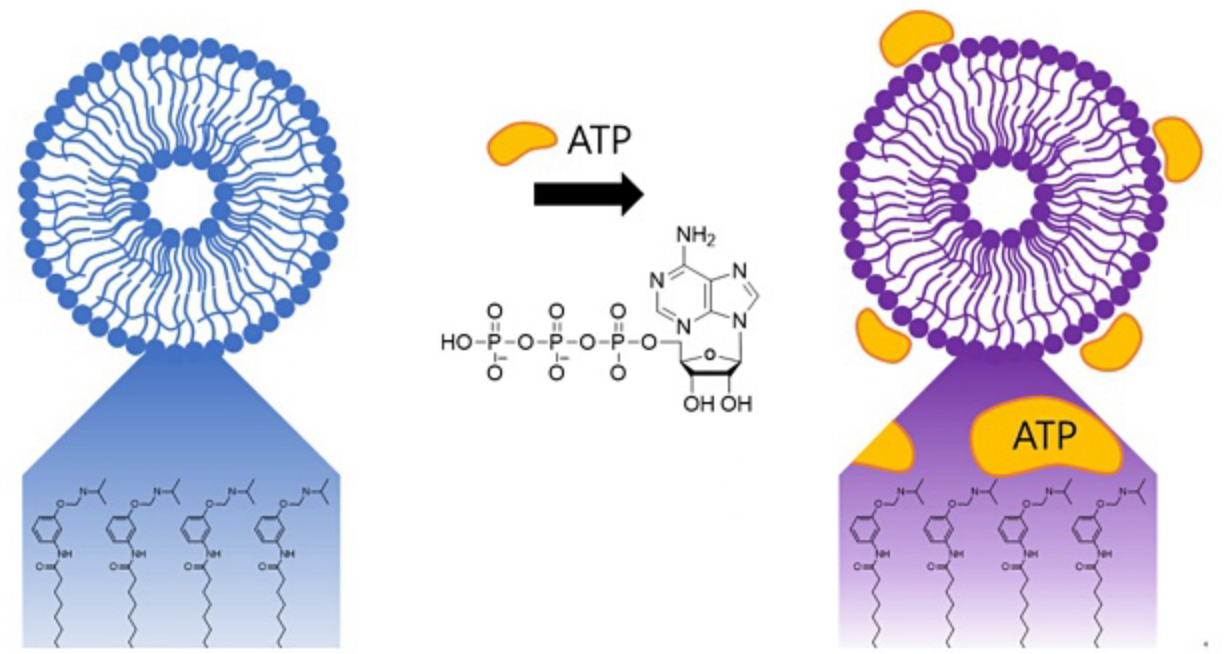

Acetylated Hyaluronic Acid-Poly(L-lactic acid) Conjugate Nanoparticles for Inhibition of Doxorubicinol Productionfrom Doxorubicin

Young-um Jo, Chae Bin Lee, Soo Kyung Bae, and Kun Na*

Macromol. Res., **28**, 67 (2020)

Doxorubicn-loaded acetylated hyaluronic acid-poly(L-lactic acid) conjugate nanoparticles (DHPs) were designed for cancer therapy and inhibition of doxorubicinol production, which is one of the major causes of doxorubicin-induced cardiotoxicity. DHPs are biocompatible and cancer-recognizable and prevent doxorubicinol production. DHP is as a new class of promising cancer therapeutic agents that may inhibit significant side effects.

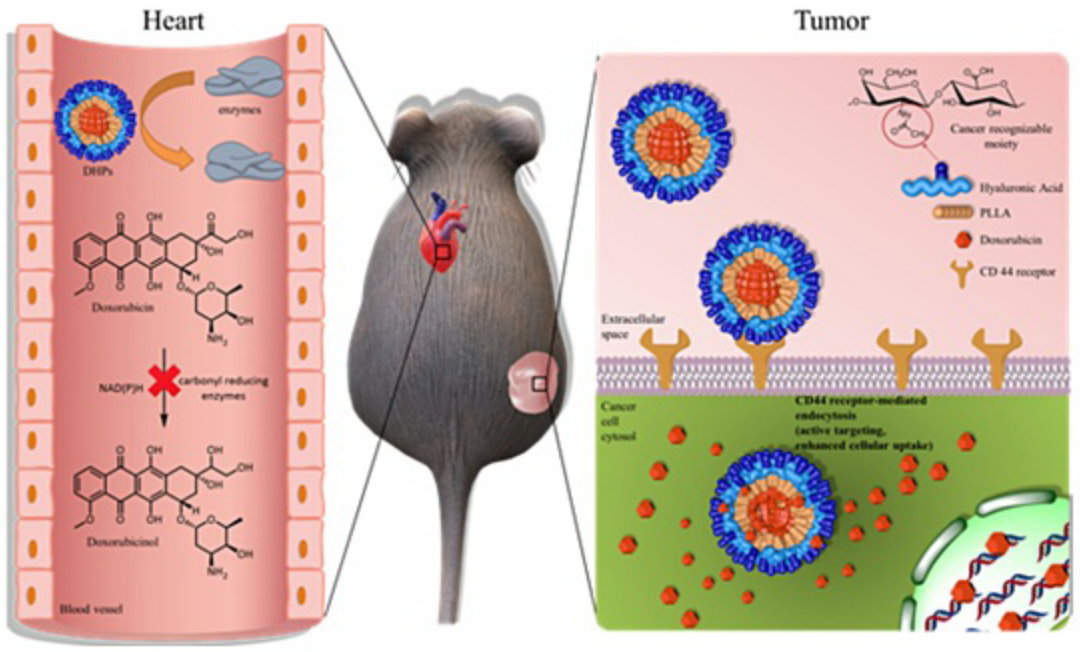

Synthesis and Properties of Benzoxazine Monomers Bearing Both 3-Methyltetrahydrophtalimide and Nitrile Groups: *Para-Para vs. Ortho-Ortho*

Yuting Wang, Sijia You, Jie Hu, and Kan Zhang*

Macromol. Res., **28**, 74 (2020)

The *ortho*-3-methytetrahydrophtalimide functional benzoxazine containing *ortho*-nitrile functionality shows both lower melting temperature and polymerization temperature compared to its *para-para* counterpart. The polybenzoxazine derived from fully *ortho*-functionalized benzoxazine monomer also exhibit advantages in terms of thermal stability and flame resistance, with a high T_{d5} of 333℃ and a low total heat release value of 21.2 kJ/g.

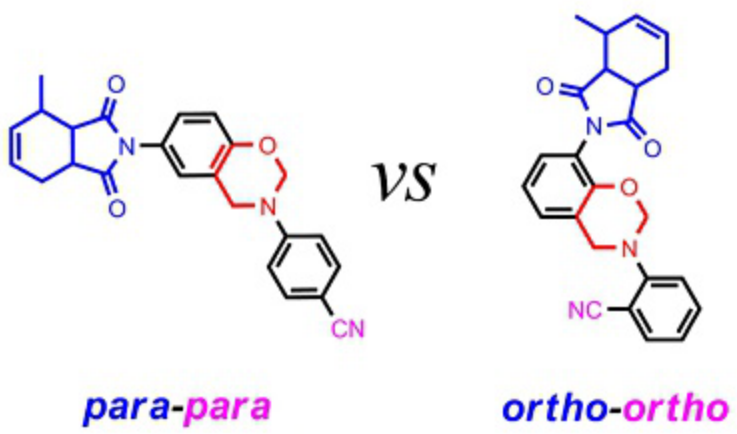

NOTE

Access to Ultra-High Molecular Weight Poly(propylene glycol)-Based Polyols Using Double Metal Cyanide Catalyst

Eun Hye Jang, Sun A Kim, Hoan Kim, Chinh Hoang Tran, Hyeong Yong Song, Kyu Hyun, Won Jin Seo, and Il Kim*

Macromol. Res., **28**, 82 (2020)

Highly pure and stereoirregular poly(propylene glycol) (PPG)-based polyols with number average molecular weight ranging from 4,800 to 43,600 g/mol are produced by using double metal cyanide catalyzed sequential ring-opening polymerizations of propylene oxide.

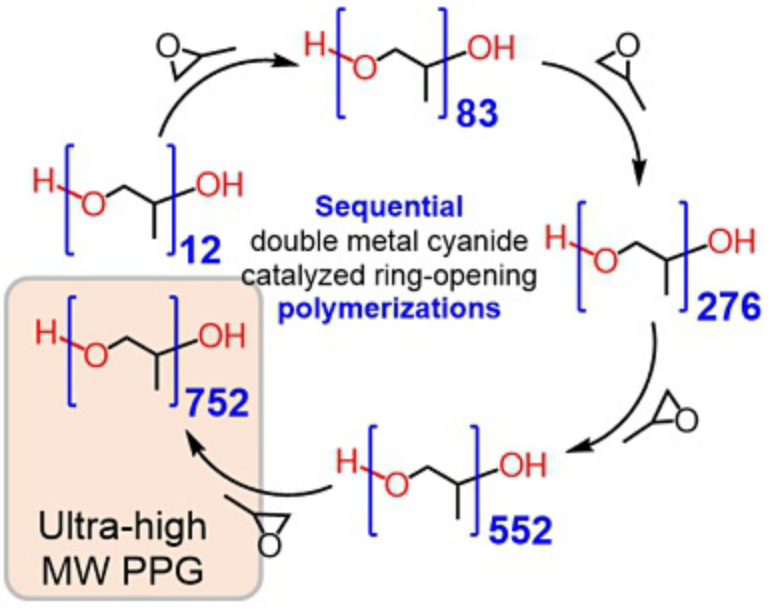

「Macromolecular Research」 목차

정기간행영문지_ 28권 2호 · 2020년 2월

COVER PAPER

Comparison of the Physical Properties and *in vivo* Bioactivities of Flatwise-Spun Silk Mats and Cocoon-Derived Silk Mats for Guided Bone Regeneration

Yei-Jin Kang, You-Young Jo, HaeYong Kweon, Weon-Sik Chae, Won-Geun Yang, Umberto Garagiola, Seong-Gon Kim*, and Horatiu Rotaru

Vol. 28, No. 2, pp 159-164 (2020) | FEB 25, 2020 | DOI 10.1007/s13233-020-8026-z

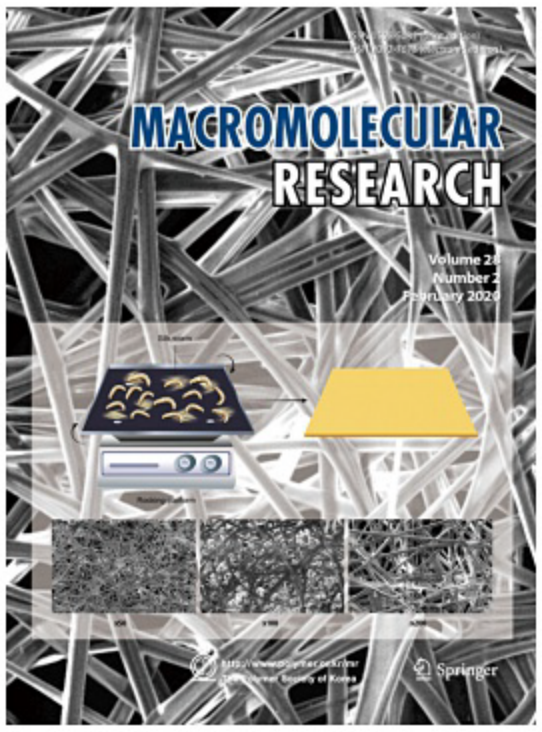

The dimensions of silkworm cocoon-originated mem-brane cannot exceed a few centimeters. Larger sized bony defects cannot be covered with this membrane. Flatwise-spun silk mats don't have size limitation. It is produced on the moving plate by disturbing the normal spinning process of the silkworms. Compared to com-mercialized silk mat, flatwise-spun silk mat showed similar physical properties and bone regeneration.

REVIEW

Strategy for Securing Key Patents in the Field of Biomaterials

Seung Hyuk Im, Chang Yong Kim, Cheol Woo Lee, Youngmee Jung, and Soo Hyun Kim*

Macromol. Res., **28**, 87 (2020)

This study suggests useful strategies for securing key biomaterial-related patents, particularly when it comes to polymeric materials. Similar patents published throughout Korea, U.S., Europe, and Japan are investigated by quantitative and qualitative analyses in regard to applicant, inventor, keyword(s), and country. The results of these analyses then become the basis for establishing patent application trends, new directions for technological development, and innovative approaches to inventing core technologies.

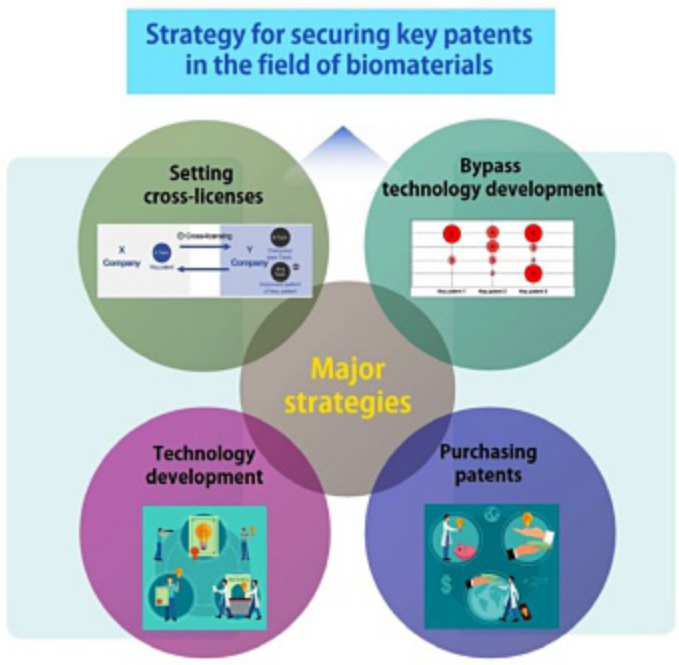

COMMUNICATION

pH-Sensitive Polymeric Micelles as the Methotrexate Carrier for Targeting Rheumatoid Arthritis

Sae Jung Moon, Dong Gil You, Yi Li, Wooram Um, Jae Min Jung, Chan Ho Kim, Byeong Hoon Oh, Jae Hyung Park*, and Doo Sung Lee*

Macromol. Res., **28**, 99 (2020)

An amphiphilic graft copolymer, composed of poly(β-amino ester)-*graft*-poly(ethylene glycol) (PAE-*g*-PEG), was self-assembled into spherical micelles in an aqueous environment. A hydrophobic methotrexate was physically loaded into the micelles. Owing to the disassociation of PAE-*g*-PEG micelles, methotrexate in the micelles was rapidly released under the mildly acidic condition, mimicking the inflamed joints in rheumatoid arthritis (RA). Overall, the pH-sensitive polymeric micelles based on PAE-*g*-PEG might be a promising candidate as the drug carrier for targeting the inflamed joint in RA.

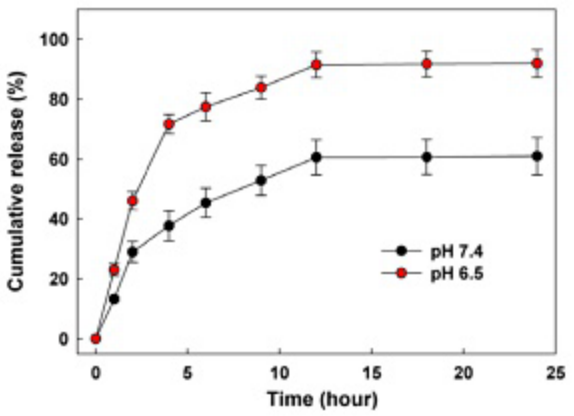

ARTICLES

PPE/Nylon 66 Blends with High Mechanical Toughness and Flame Retardancy

Do Kyun Kim, Albert S. Lee, Bum Ki Baek, Kwang Ho Song, Soon Man Hong, and Chong Min Koo*

Macromol. Res., **28**, 103 (2020)

Poly(2,6-dimethyl-1,4-phenylene ether) (PPE)/Nylon 66 blend with high mechanical toughness and flame retardancy was prepared by introduction of fumaric acid-grafted PPE (PPE-*g*-FA) compatibilizer and no-halogenic flame retardant.

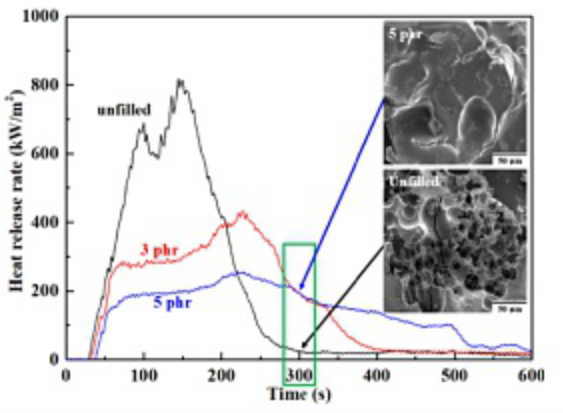

Pretreatment of Microfibrillated Cellulose on Polylactide Composites

Hyo Jae Lee, Yeon Sung Ryu, Ick Soo Kim, and Seong Hun Kim*

Macromol. Res., **28**, 110 (2020)

Microfibrillated cellulose (MFC) has attracted increasing applications as fully bioderived nanocomposites. Polymer composites from polylactide (PLA) and MFC were prepared using two different fiber preparation methods. First, freeze-dried MFC was prepared and directly mixed with PLA in an internal mixer. Second, the MFC premixed with PLA in an organic solvent was prepared, followed by an internal mixer for another composite. In addition, grafting cellulose on PLA using a compatibilizer was performed. In this research, composites containing 10 wt% MFC were used to investigate the influence of processing and compatibilizer on the mechanical and thermal properties. The processing procedure had a great influence on the mechanical and physical properties. The tensile strength was increased with filler loading and showed different values depending on premixing step. The storage modulus and loss tangent confirmed that the compatibilizer acted as a bridge between filler and matrix and enhanced mechanical properties. This experiment was conducted to compare the effect of pretreatment on the change of mechanical and thermal properties by using freeze-dried cellulose and cellulose suspension substituted with an organic solvent.

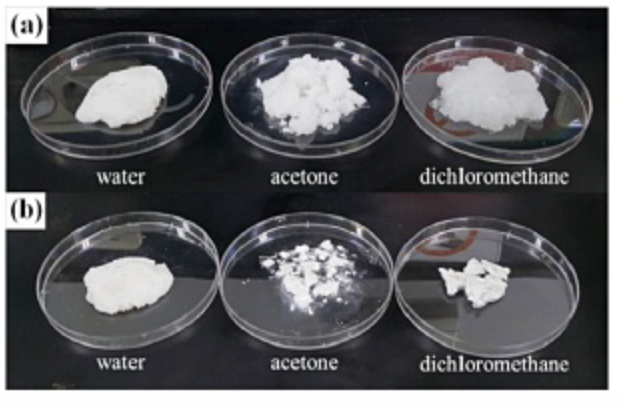

Improvements of the Electrical Conductivity and EMI Shielding Efficiency for the Polycarbonate/ ABS/Carbon Fiber Composites Prepared by Pultrusion Process

Seung Chan Ryu, Jae Young Kim, Choonglai Cho, and Woo Nyon Kim*

Macromol. Res., **28**, 118 (2020)

The polycarbonate/poly(acrylonitrile-butadiene-styrene) (70/30)/carbon fiber (CF) composite prepared by the pultrusion process showed higher electromagnetic interference (EMI) shielding efficiency of 37.6 dB compared to the composite prepared by screw extrusion of 6.8 dB at 10 GHz. The increase in the shielding efficiency of electromagnetic wave by 30.8 dB was due to the increased fiber length when the composite was prepared by the pultrusion process.

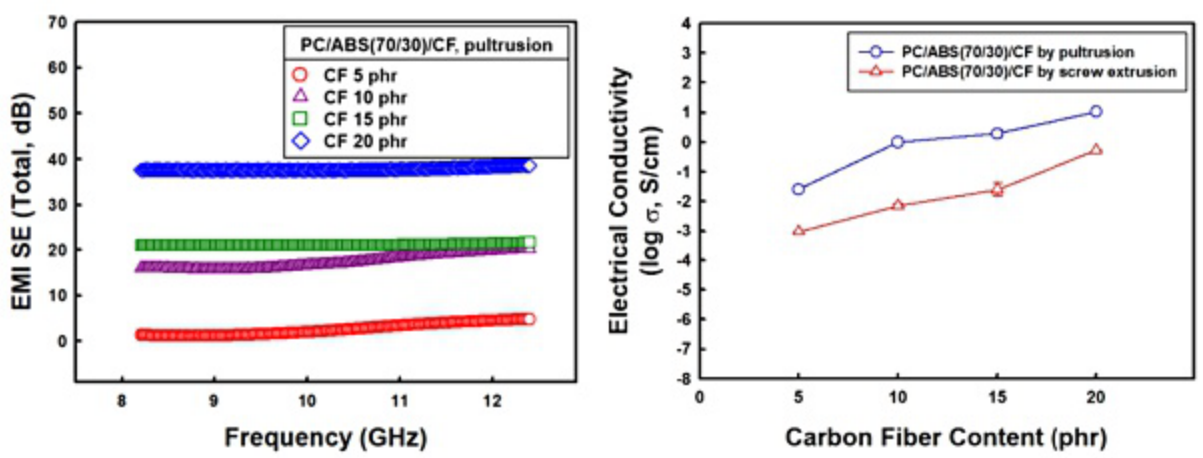

Tuning with Phosphorylcholine Grafts Improves the Physicochemical Properties of PLL/pDNA Nanoparticles at Neutral pH

Juliana Semensato, Júlio Cesar Fernandes, Mohamed Benderdour, Vera Aparecida de Oliveira Tiera, Aline Margarete Furuyama Lima, and Marcio José Tiera*

Macromol. Res., **28**, 126 (2020)

Tuning with phosphorylcholine grafts improves the physicochemical properties of PLL/pDNA nanoparticles at neutral pH.

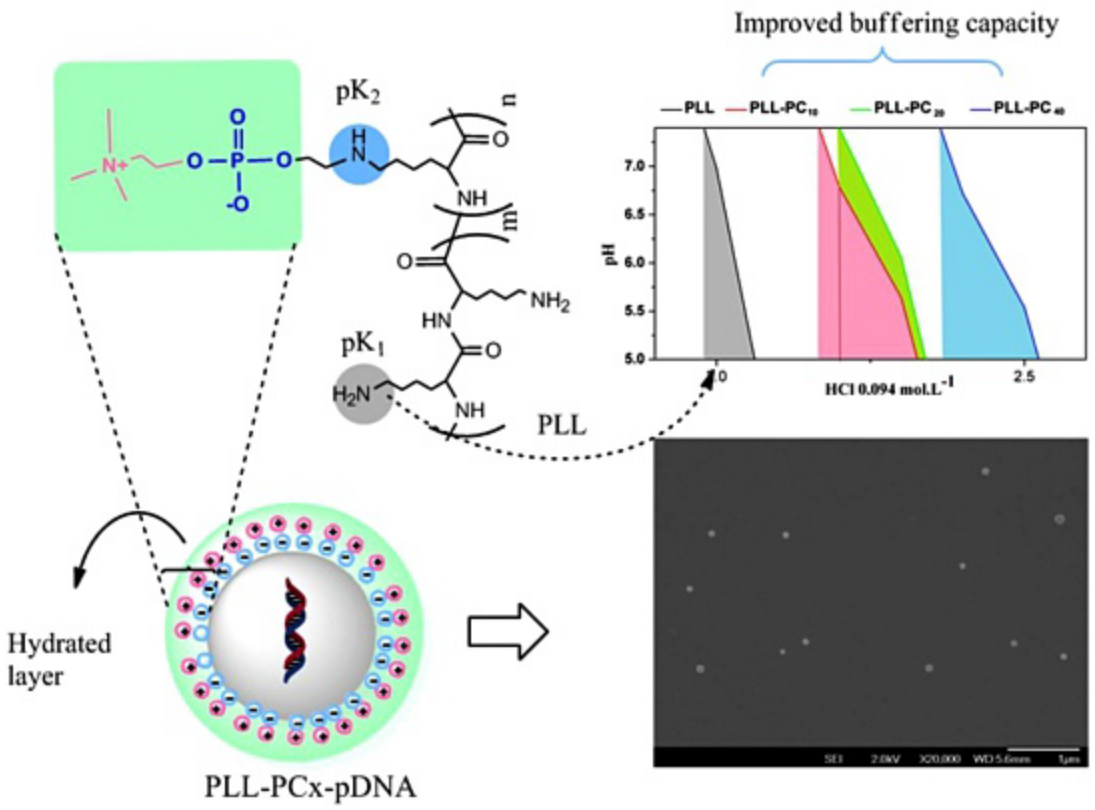

Insertion of a Cardo Structure into a Polyurethane Framework Using a pH Indicator and Its Impact on Tensile and Shape Memory Properties

Yong-Chan Chung, Dong Eui Kim, Jae Won Choi, and Byoung Chul Chun*

Macromol. Res., **28**, 136 (2020)

Perpendicular cardo structural units were inserted into a polyurethane (PU) framework from the pH indicator (phenolphthalein (PP), phenol red (PR), or bromocresol green (BG)) sharing a triphenylmethyl group. The breaking tensile stress, shape recovery capability at 0 °C, and low-temperature flexibility of the BG-PU series have notably improved. The inserted pH indicator moieties did not show the color change under different pH conditions because the isomerization under basic conditions was blocked.

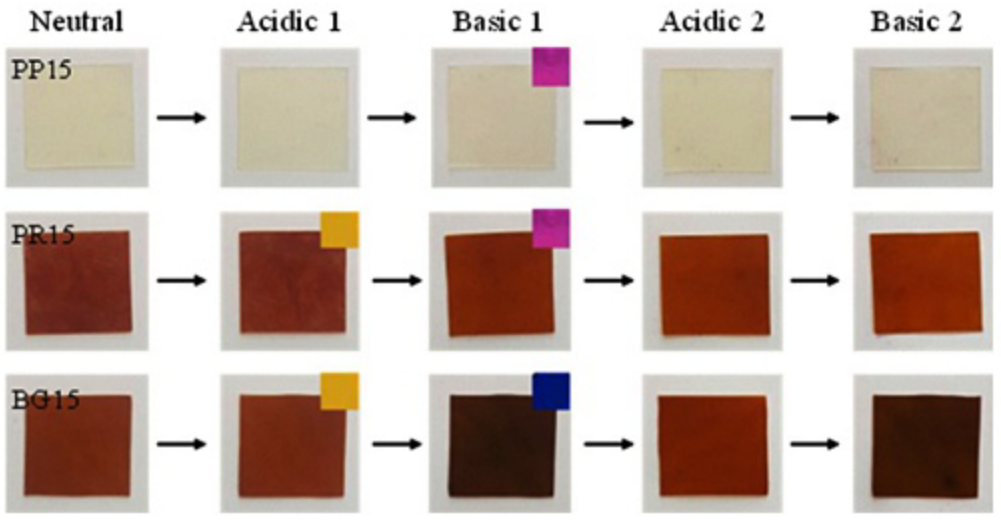

Enhancing Microalgal Biomass Productivity in Floating Photobioreactors with Semi-Permeable Membranes Grafted with 4-Hydroxyphenethyl Bromide

Kwangmin Kim, Z-Hun Kim, Hanwool Park, Yunwoo Lee, Kihyun Kim, Sungmo Kang, Sang-Min Lim, and Choul-Gyun Lee*

Macromol. Res., **28**, 145 (2020)

4-Hydroxyphenethyl bromide (4-HPB) grafted semi-permeable membranes (SPMs) were fabricated to reduce biofouling and improve biomass productivity. 4-HPB grafted SPMs could lower hydrophobicity and reduce the degree of biofouling. Ion and water permeabilities of 4-HPB grafted SPMs were improved. Eventually, 4-HPB grafted SPMs enhanced biomass productivity of *Tetraselmis* sp.

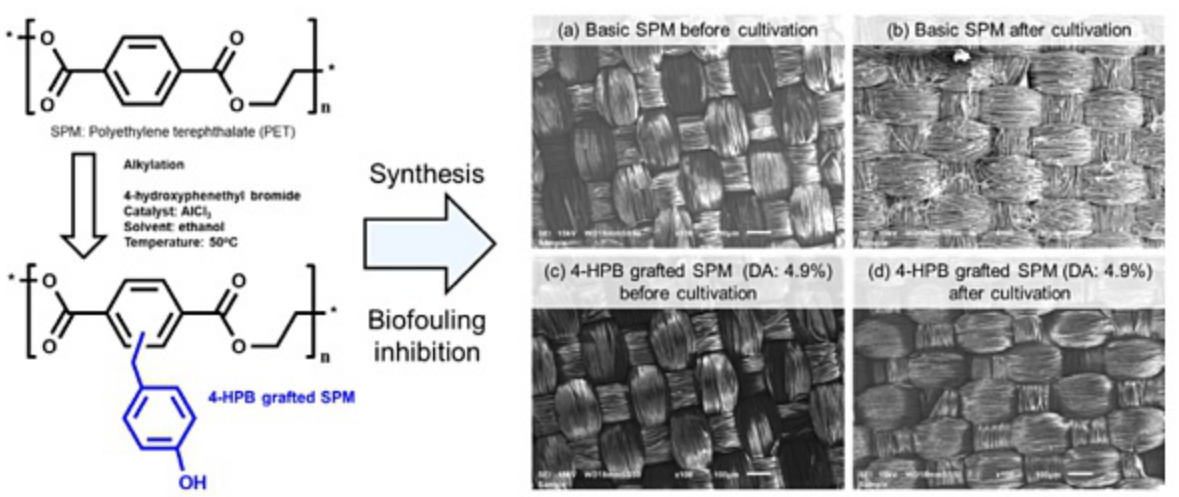

Novel Organic/Inorganic Hybrid Star Polymer Surface-Crosslinked with Polyhedral Oligomeric Silsesquioxane

Jingyan Zhang*, Dong Si, Shifeng Wang, Hao Liu, Xiaoming Chen, Haiou Zhou, Mingdi Yang, and Guoying Zhang*

Macromol. Res., **28**, 152 (2020)

An approach for the preparation of organic/inorganic hybrid multiarm star polymer dually cross-linked within the core and surface regions was accomplished *via* surface "click" crosslinking of a core-crosslinked polymer with octafunctional polyhedral oligomeric silsesquioxane (POSS). On average, the obtained hybrid polymer possesses a cross-linked poly-divinylbenzene (PDVB) inner core, ~14 linear PS arms (the M_W per arm of 5.1 kDa), and ~4-5 polyhedral oligomeric silsesquioxane (POSS) moieties at outer surface.

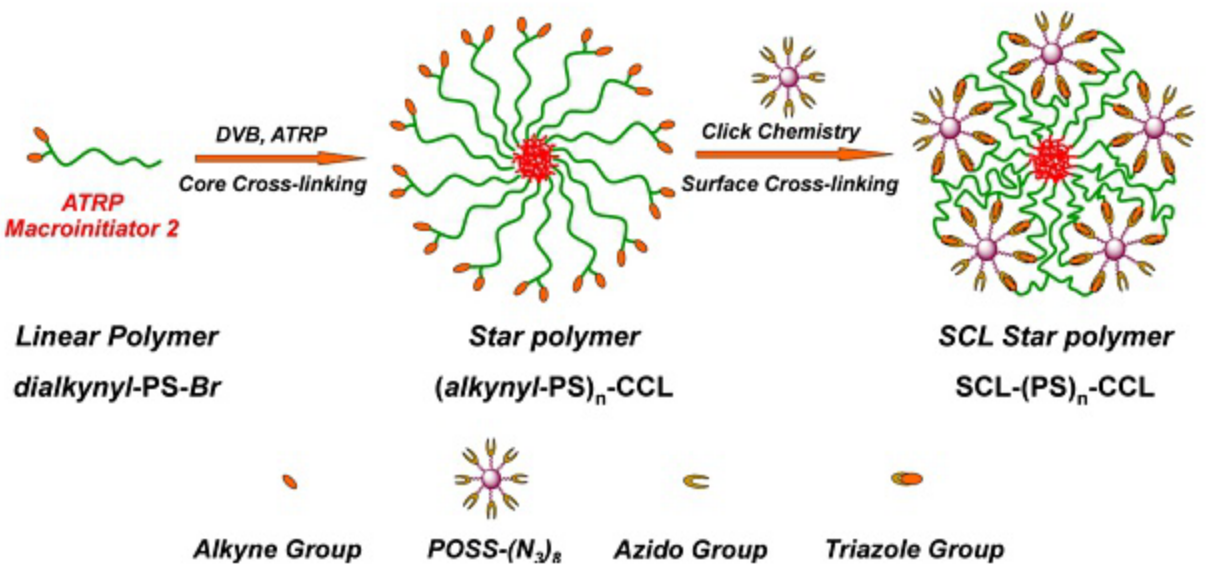

Comparison of the Physical Properties and *in vivo* Bioactivities of Flatwise-Spun Silk Mats and Cocoon-Derived Silk Mats for Guided Bone Regeneration

Yei-Jin Kang, You-Young Jo, HaeYong Kweon, Weon-Sik Chae, Won-Geun Yang, Umberto Garagiola, Seong-Gon Kim*, and Horatiu Rotaru

Macromol. Res., **28**, 159 (2020)

Cover Paper

The bone volume (BV) after applying a flatwise-spun silk mat was similar to that after applying a cocoon-derived commercialized silk mat (TDI). Both groups showed a significantly higher BV compared to an unfilled control group (P<0.05). Accordingly, flatwise-spun silk mats had similar properties as TDIs for GBR.

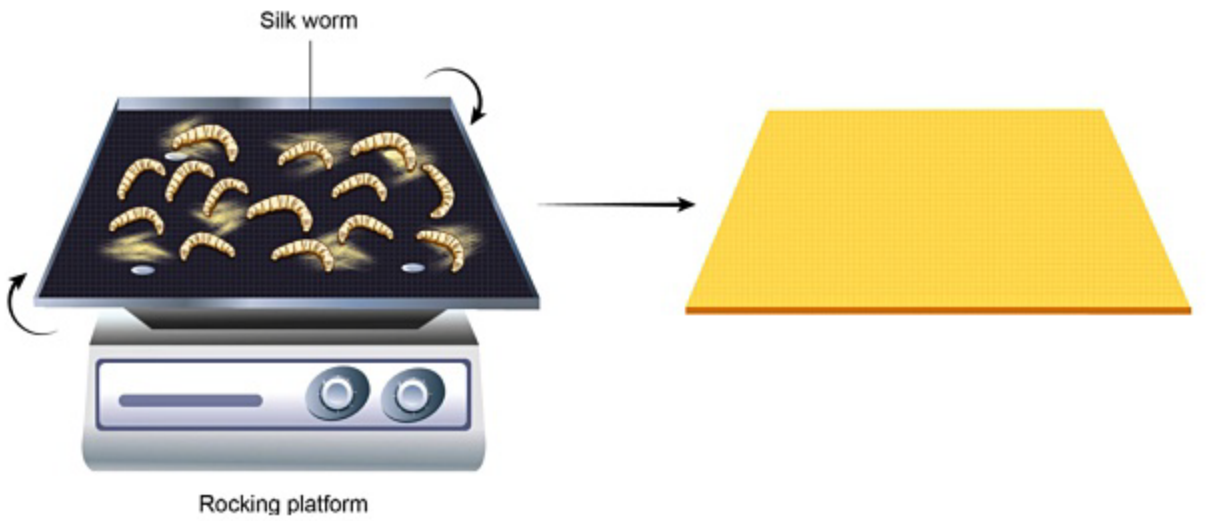

Eco-Friendly Nanocellulose Embedded Polymer Composite Foam for Flame Retardancy Improvement

Hansu Kim, Juhyuk Park,
Kyung Suh Minn, Jae Ryoun Youn*,
and Young Seok Song*

Macromol. Res., **28**, 165 (2020)

A unique flame retardant foam made of polyurethane composite is engineered. Simultaneous incorporation of the silylated nanocellulose and a conventionally available flame retardant into the polymer matrix brings out synergistic performance of flame retardancy, reduces environmental-burden upon burning, and ensures other good thermal and mechanical properties. The underlying mechanisms of these results are explained with various analytical methods.

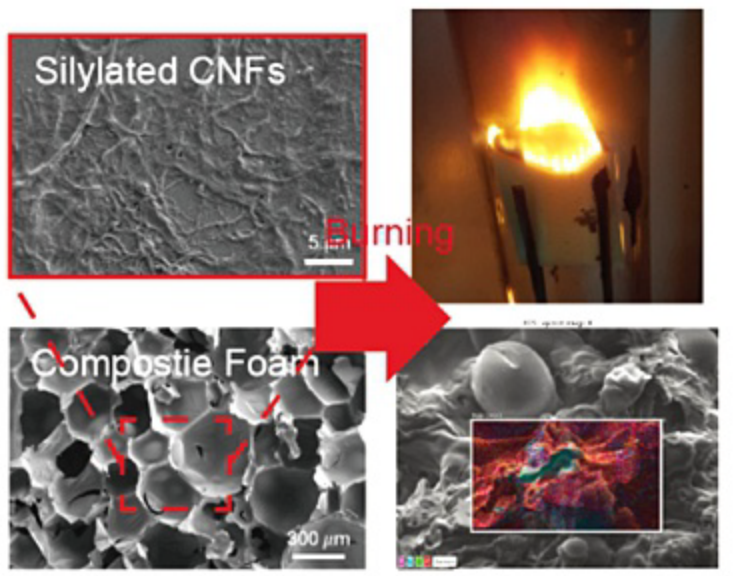

Surface Modification of Polystyrene Beads with Sulfonamide Derivatives and Application to Water Softening System

Seong Ik Jeon, In Jae Chung,
and Cheol-Hee Ahn*

Macromol. Res., **28**, 172 (2020)

Removal of magnesium and calcium cations in water, called water softening, is an important procedure for industrial use. Herein, sulfonamide-derived cation capturing system was suggested as an alternative. Among the surface-treated sulfonamide derivatives, glycine-conjugated sulfonamide group, which had 0.90±0.01 mmol/g of ion capturing capacity and rapidly regenerated at pH 5.0, was found to be most appropriate for water softening application.

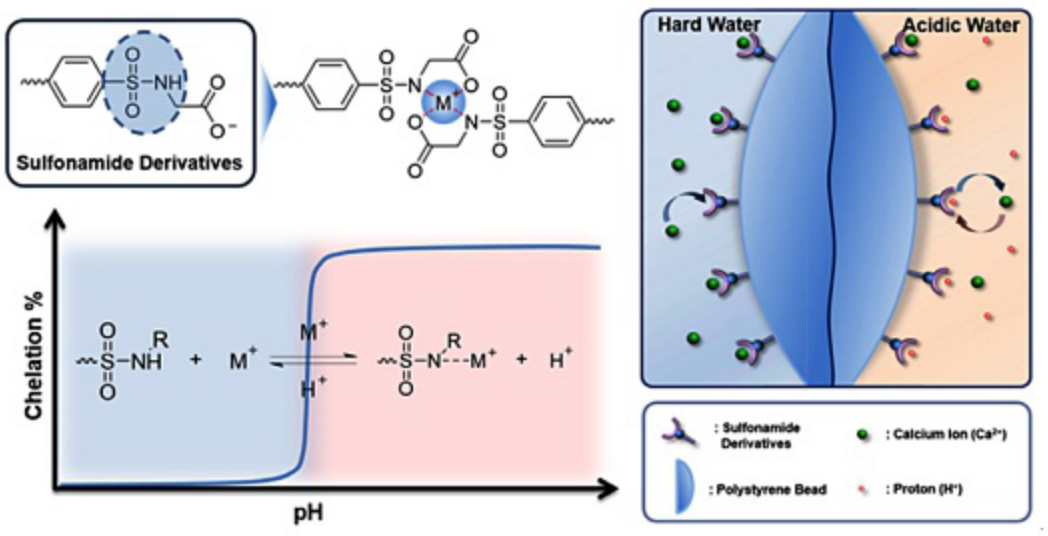

A New Benzodithiophene Based Donor-Acceptor π-Conjugated Polymer for Organic Solar Cells

Saripally Sudhaker Reddy,
Um Kanta Aryal, Hyunjung Jin,
Thavamani Gokulnath,
Durga Gayathri Rajalapati,
Kakaraparthi Kranthiraja,
Sung Tae Shin, and Sung-Ho Jin*

Macromol. Res., **28**, 179 (2020)

A new π-conjugated polymer (P1) is synthesized as the photoactive donor for both non-halogenated and halogenated solvent processed organic solar cell (OSC). The incorporation of side chain octyl group on the acceptor unit of donor polymer had notable influence on the photoactive layer morphology. The enhanced morphology of the P1:$PC_{71}BM$ active layer leads to an increased interfacial area and improved charge carrier mobility which in turn helps in improving the OSC device performance after solvent additive.